

Stick-slip versus smooth sliding in the multicontact frictional interface

O.M. Braun*

Institute of Physics, National Academy of Sciences of Ukraine, 46 Science Avenue, 03028 Kiev, Ukraine

(Dated: October 21, 2014)

The stick-slip and smooth sliding regimes of motion for the multicontact frictional interface are studied within the earthquakelike model, and the conditions when stick-slip appears are determined.

PACS numbers: 81.40.Pq; 46.55.+d; 61.72.Hh

Introduction. The regime of motion of the frictional interface—stick-slip or smooth sliding—is a rather old but very important problem in tribology [1, 2]. In some situations (for example, for violin playing) stick-slip is a desirable regime, but in majority of cases (e.g., for windshield wiper, car engine operation, earthquakes, etc.) the stick-slip has to be avoided or suppressed at least. These two regimes, the stick-slip and smooth sliding, and the transitions between them are traditionally described by a phenomenological theory based on the “velocity weakening” assumption [1, 2]: if the friction force decreases when the sliding velocity grows, the motion may become unstable and could switch to stick-slip, either periodic or irregular (intermittent) motion. The theory predicts that generally stick-slip emerges for a soft system and low driving velocities. However, a general physical theory of this problem is still lacking.

In the present work we consider a multicontact interface (MCI), when the contact between two surfaces is due to many “frictional” contacts (asperities, bridges, etc.)—a rather general situation in tribology. The MCI may be described by an earthquakelike (EQ) model (based on the famous spring-and-block Burridge and Knopoff model [3] and adopted to the frictional interface, e.g., in Refs. [4–6]), which allows an analytical description using the master equation (ME) approach [7, 8]. The stick-slip motion in the MCI may appear, *if and only if* two ingredients are incorporated into the model: the elastic instability of the system and ageing of the contacts [9, 10]. The aim of the present work is to find the conditions when the stick-slip regime emerges in the multicontact interface.

EQ model and ME approach. The EQ model is shown schematically in Fig. 1 (inset). The top block (the slider) is coupled with the bottom block (the base; we assume it to be rigid and fixed for the sake of simplicity) by N frictional contacts. Each contact is characterized by a shear force $f_i = kx_i$, where k is the contact stiffness and x_i is its strain, and by a threshold value f_{si} . The contact stretches elastically so long as $|f_i| < f_{si} = kx_{si}$, but becomes plastic and breaks when the threshold is exceeded. When a contact breaks at $|f_i| = f_{si}$, its stretching drops to $x_i \sim 0$, and evolution continues from there, with a new

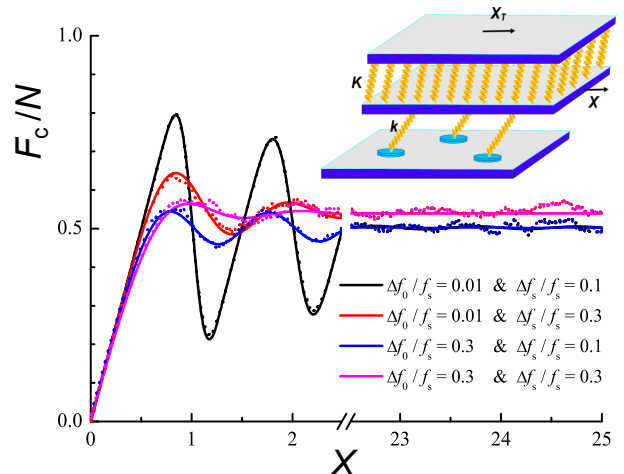


FIG. 1: (color online): Rigid motion of the slider: the total force from contacts F_c as function of the slider displacement X for two initial distributions $\Delta f_0/f_s = 0.01$ and 0.3 and two values of the threshold distribution $\Delta f_s/f_s = 0.1$ and 0.3 (see legend). Solid curves describe solutions of the master equation, dotted curves show results of simulation of the earthquakelike model with $N = 10^3$ contacts; the latter fluctuate with the amplitude $\propto N^{-1/2}$. Inset: the earthquakelike model.

value for its successive breaking threshold assigned. The contact thresholds are characterized by some distribution $P_c(x)$ which is determined by interface structure, e.g., by surface roughness. In what follows we assume that the normalized probability distribution of values of the stretching thresholds x_{si} at which contacts break, $P_c(x)$, has the Gaussian shape centered at $x = x_s = f_s/k$ with a dispersion $\Delta x_s = \Delta f_s/k$.

The EQ model, being a cellular automaton model, allows a numerical study only. Rather than studying its evolution by numerical simulation, it is possible to describe it analytically with the ME approach [7, 8]. To describe the evolution of the system, we introduce the distribution $Q(x; X)$ of the contact stretchings x_i when the sliding block is at position X . Evolution of the system is described by the integro-differential equation (the master equation)

$$\left[\frac{\partial}{\partial X} + \frac{\partial}{\partial x} + P(x) \right] Q(x; X) = R(x) \Gamma(X), \quad (1)$$

*E-mail: obraun.gm@gmail.com; Web: <http://www.iop.kiev.ua/~obraun>

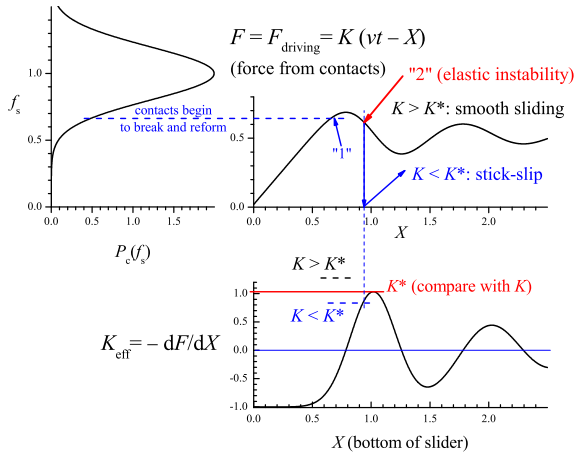


FIG. 2: (color online): Elastic instability.

where

$$\Gamma(X) = \int_{-\infty}^{\infty} d\xi P(\xi) Q(\xi; X) \quad (2)$$

and

$$P(x) = P_c(x)/J_c(x), \quad J_c(x) = \int_x^{\infty} d\xi P_c(\xi). \quad (3)$$

Then, the total force experiences by the slider from the interface is given by

$$F_c(X) = Nk \int_{-\infty}^{\infty} dx x Q(x; X). \quad (4)$$

A typical dependence of the total force F_c from the contacts on the slider displacement X is shown in Fig. 1. Except the exotic case of delta-function distribution of thresholds, the system always approaches the steady state with the distribution $Q_s(x)$ in the limit $X \rightarrow \infty$, where the function $F_c(X)$ takes the constant value $F_k \approx \frac{1}{2} N f_s$. The value F_k corresponds to the kinetic friction force, while the maximum of the $F_c(X)$ dependence is associated with the static friction force. We emphasize that the shape of the function $F_c(X)$ depends on the initial distribution $Q_i(x)$ of the system: the strongest initial oscillations of $F_c(X)$ are achieved for the delta-function initial distribution $Q_i(x) = \delta(x)$, while in the case of $Q_i(x) = Q_s(x)$ the force is independent of X , $F_c(X) = F_k$.

Elastic instability. Now let us consider a system where the top block is driven with a velocity v_d through a spring of elastic constant K so that the driving force is $F_d = K(v_d t - X)$; the role of spring may be played by the elasticity of the slider itself, if the driving force is applied to its top surface. For adiabatically slow driving, $v_d \rightarrow 0$, if one starts from the relaxed state at $t = 0$, the increasing driving force F_d has to be compensated by the force F_c from the interface contacts, so that they grow together at the beginning. However, when the slider displacement

X approaches the threshold value x_s , the contacts start to break (see the point marked by “1” in Fig. 2), the growth of F_c becomes slower and then changes to decreasing as shown in Fig. 2. If the driving spring is stiff enough, $K > K^*$, the driving force F_d will adjust itself to the changed value of F_c . For a soft system, however, at some point X^* (marked by “2” in Fig. 2) the two forces cannot compensate one another, an elastic instability occurs, and the slider will undergo an accelerated motion until the forces will compensate one another again.

An alternative explanation of the elastic instability follows from the consideration of the effective potential energy of the system. The total force applied to the bottom of the sliding block, which determines its displacement X , is the sum of the applied force and the friction force, $F_{\text{tot}}(X) = K(v_d t - X) - F_c(X)$. It can be viewed as derived from the effective potential, $F_{\text{tot}}(X) = -dV_{\text{eff}}(X)/dX$, where

$$V_{\text{eff}}(X) = \frac{1}{2} K(v_d t - X)^2 + \int_0^X d\xi F_c(\xi). \quad (5)$$

The slider state at the position X is stable if

$$d^2 V_{\text{eff}}(X)/dX^2 = K + dF_c(X)/dX > 0 \quad (6)$$

and unstable otherwise. If we introduce the effective interface stiffness

$$K_{\text{eff}}(X) = -dF_c(X)/dX, \quad (7)$$

then the slider motion becomes unstable for displacements X where $K_{\text{eff}}(X) > K$. Thus, the critical stiffness is defined by

$$K^* = \max K_{\text{eff}}(X). \quad (8)$$

If $K > K^*$, the system is stiff and does not undergo elastic instability.

The critical value K^* depends on *two factors*: on the threshold distribution $P_c(x)$ and on the initial distribution $Q_i(x) = Q(x; X = 0)$; the maximum value of K^* is achieved for the delta-function initial distribution $Q_i(x) = \delta(x)$, while the minimal value—equal to zero—for the stationary distribution $Q_i(x) = Q_s(x)$. For the Gaussian shape of the initial and threshold distributions, the dependence of K^* on the model parameters is shown in Fig. 3; roughly it may be described by the formula

$$K^* \approx Nk f_s / (\Delta f_s + \Delta f_0), \quad (9)$$

where $\Delta f_0 = k \Delta x_0$ is the dispersion of the initial distribution.

Dynamics. The elastic instability is the necessary but not sufficient condition for stick-slip to emerge; the second necessary condition is the ageing of contacts—an increase of contact thresholds with their lifetime. Indeed, if after breaking the newborn contacts obtain thresholds from the same distribution $P_c(x)$, then the dependence $F_c(X)$ will remain approximately unchanged despite the

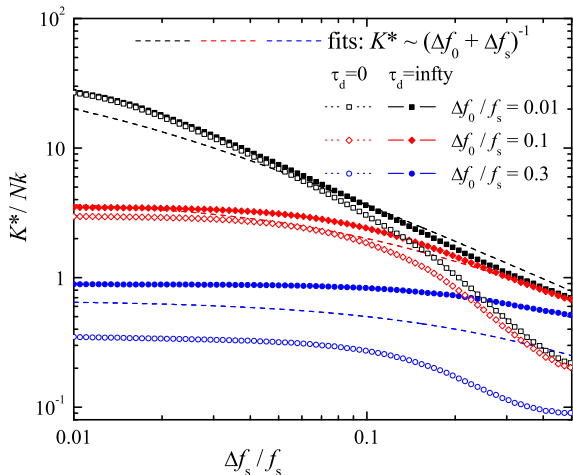


FIG. 3: (color online): The critical stiffness K^* as function of the threshold dispersion Δf_s for different values of the initial state distribution Δf_0 .

fact that the slider motion is accelerated in the interval where $K_{\text{eff}}(X) > K^*$ as demonstrated in Fig. 4a.

The simplest way to incorporate contact ageing is to introduce a delay time τ_d , i.e., to assume that after breaking the contact reappears after some time τ_d (thus, for a lifetime shorter than τ_d the threshold is zero). Within the ME approach, the delay effects may be included as follows. Let N be the total number of contacts, N_c be the number of attached (pinned) contacts, $N_f = N - N_c$ be the number of detached (sliding) contacts, and $v = \dot{X}$ be the sliding velocity. The fraction of contacts that detach per unit displacement of the sliding block is $\Gamma(X) = \int dx P(x; X) Q(x; X)$, i.e., when the slider shifts by ΔX , the number of detached contacts changes by $N_c \Gamma \Delta X$, so that $N_f = \Gamma v \tau_d N_c$. Using $N_c + N_f = N$, we obtain $N_c = N/(1 + \Gamma v \tau_d)$ and $N_f = N \Gamma v \tau_d / (1 + \Gamma v \tau_d)$. Introducing $\bar{x} = 1/\Gamma$ and $\bar{v} = \bar{x}/\tau_d$, we can write

$$N_c = N / (1 + v/\bar{v}). \quad (10)$$

The pinned contacts produce the force $F_c(X)$ defined above by Eq. (4) (with N_c instead of N) by solution of the master equation.

The slider motion is described by the equation

$$M\ddot{X}(t) + M\eta\dot{X}(t) = K[v_d t - X(t)] - F_c(X(t)), \quad (11)$$

where M is the slider mass and the coefficient η describes the rate of energy dissipation (e.g., due to phonons emitted inside the slider); the latter is responsible for decaying ringing oscillations at stick-slip and thus can be found experimentally. Figure 4c shows that for a large enough delay time $\tau_d > \tau^*$ the slider motion corresponds to stick-slip provided $K < K^*$.

To find the critical delay time τ^* , let us consider the slider trajectory just after the critical displacement X^*

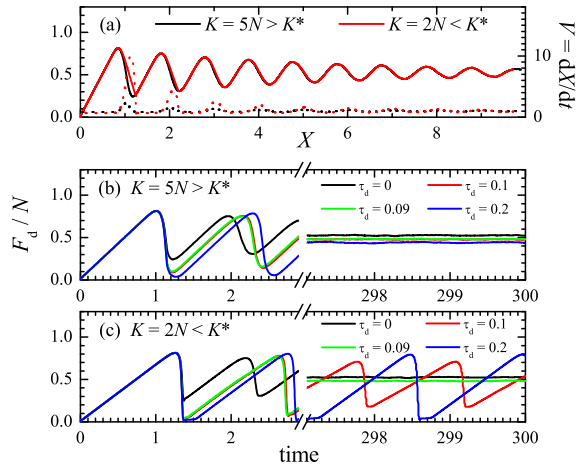


FIG. 4: (color online): (a) Dependence of the driving force F_d (solid) and the slider velocity \dot{X} (dotted curves, right axes) on the slider displacement X for two values of the spring constant: $K/N = 5$ (above the critical value $K^*/N = 3.59$) and $K/N = 2$ (when the elastic instability occurs). (b) Dependence of F_d on time for different values of the delay time $\tau_d = 0, 0.09, 0.1$ and 0.2 (see legend) for the spring constant $K/N = 5$ and (c) $K/N = 2$. The parameters are the following: $f_s = 1$, $\Delta f_s = 0.1$, $\Delta f_0 = 0.01$, $k = 1$, $v_d = 1$, $M/N = 10^{-4}$ (so that $\Omega = (K/M)^{1/2} = 223.6$ for $K/N = 5$ and $\Omega = 141.4$ for $K/N = 2$), $\eta = 200 \sim \Omega$, and $N = 10^4$.

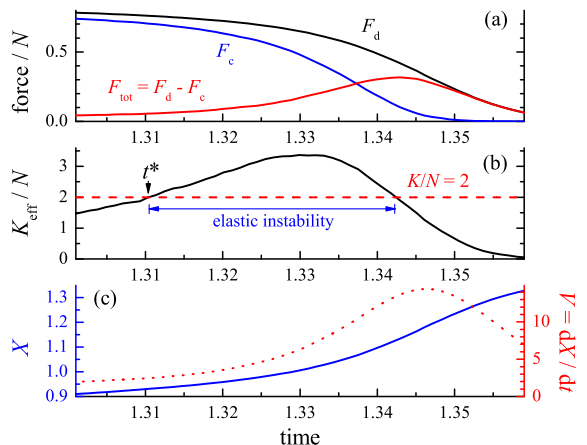


FIG. 5: (color online): System dynamics at/after the elastic instability for $K/N = 2$ and $\tau_d = \infty$ (other parameters as in Fig. 4).

(the point “2” in Fig. 2), when the elastic instability occurs and the motion becomes unstable. The system dynamics is shown in Fig. 5. Before the instability, $t < t^*$, the two forces, the driving force F_d and the force from contacts F_c , approximately compensate one another, and the slider moves with a constant velocity, $\dot{X} \approx v_d$. After t^* , however, the forces become unbalanced, the difference $F_{\text{tot}} = F_d - F_c$ grows with $\Delta t = t - t^*$ (see Fig. 5a), and the slider undergoes an accelerated motion with increasing velocity (Fig. 5c). As was found in Ref. [10], for $t > t^*$

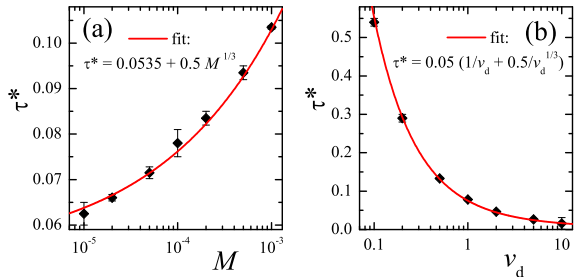


FIG. 6: (color online): (a) The critical delay time τ^* as function of the slider mass M at constant $v_d = 1$, and (b) τ^* as function of the driving velocity v_d at fixed $M = 10^{-4}$. $K/N = 2$ and $\eta = 0.3\Omega$; other parameters as in Fig. 4.

the slider position changes as

$$\Delta X(t) \approx v_d \Delta t \left[1 + \frac{1}{6} (\Omega \Delta t)^2 \right], \quad (12)$$

where $\Omega^2 = K/M$. When the delay time is nonzero, the slider slips a distance $\Delta X_d = \Delta X(\tau_d)$ during τ_d . Therefore, if $\Delta X_d \gtrsim 0.5 \Delta x_s$, then most of the contacts break and reform with $f \sim 0$ during the time τ_d , and the distribution of stresses shrinks, $Q(x; t^* + \tau_d) \rightarrow \delta(x)$. Thus, the next cycle begins with a narrow stress distribution, and the elastic instability will occur again—that is stick-slip.

The critical delay time τ^* may be estimated from Eq. (12); for $\Omega \tau^* \ll 1$ this gives $\tau^* \approx \Delta x_s / v_d$, while for $\Omega \tau^* \gg 1$ it leads to the relation $\tau^* \approx (6 \Delta x_s M / K v_d)^{1/3}$. These relations agree well with the numerics (see Fig. 6) which suggests the dependences $\tau^*(M) \approx A_1 + A_2 M^{1/3}$ and $\tau^*(v_d) \approx A_3 v_d^{-1} + A_4 v_d^{-1/3}$, where $A_{1...4}$ are numerical constants. Numerics shows also that τ^* increases with the damping coefficient η ; τ^* also depends on the parameters Δf_s and Δf_0 .

As follows from Fig. 6b, for a fixed nonzero value of the delay time τ_d the system should undergo a transition from smooth sliding to stick-slip when the driving velocity increases. Such transition is demonstrated in Fig. 7a. The system exhibits hysteresis: when the driving velocity increases, the smooth to stick-slip transition occurs at some velocity v_1 , while when v_d decreases, the stick-slip to smooth sliding transition occurs at a lower velocity v'_1 . The hysteresis takes place because, as mentioned above, the criterion of the elastic instability to occur, depends on the initial distribution for a given cycle of stick-slip, which is different in the v_d increasing and decreasing processes. Thus, depending on the system initial state and the model parameters, the motion corresponds to either stick-slip or smooth sliding. These regimes are stable, both correspond to regular motion, in particular, the stick-slip motion is strictly periodic.

The simplest “delay time” variant of ageing predicts the transition from smooth sliding to stick-slip with the increase of the driving velocity, as indeed was observed experimentally [11]. More traditional, however, is the opposite scenario, when stick-slip is observed at low v_d

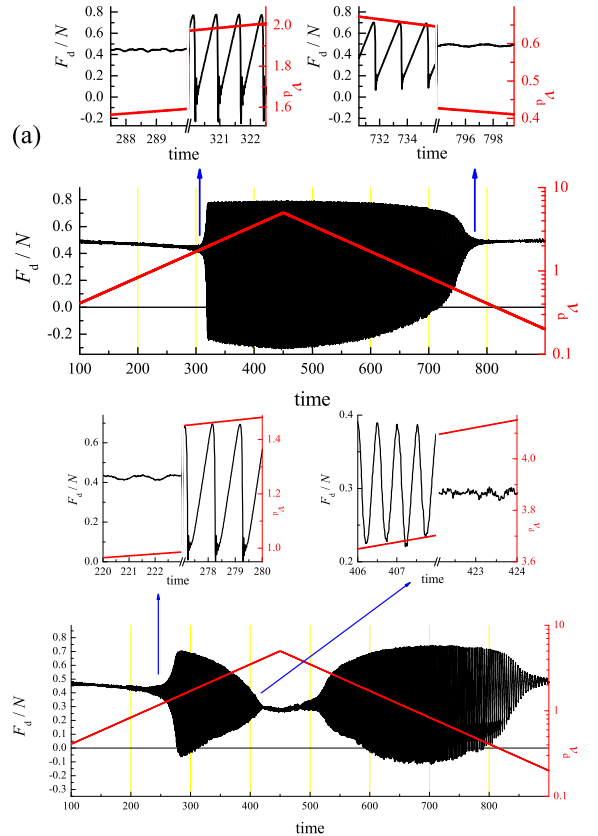


FIG. 7: (color online): The friction force as function of time, when the driving velocity v_d (thick red line, right axes) continuously increases/decreases with time. (a) Fixed value of the delay time $\tau_d = 0.1$. (b) Delay time takes random values from Gaussian distribution with $\langle \tau_d \rangle = 0.2$ and $\Delta \tau_d = 0.12$. Insets show the smooth to stick-slip transitions. $K/N = 2$, $M = 10^{-4}$ and $\eta = 0.3\Omega$; other parameters as in Fig. 4.

and changes to smooth sliding when the driving velocity increases [1, 2]. The EQ model does demonstrate such a behavior, if we assume that the parameter τ_d takes random values from some distribution $P_\tau(\tau_d)$ with a dispersion $\Delta \tau_d$, as shown in Fig. 7b. Moreover, in this case one may expect an irregular stick-slip as well [12–14]. This second transition occurs because the elastic instability disappears at large velocities—after slip phase at the stick-slip event, the newborn contacts have the distribution with the dispersion $\Delta x \propto v_d \Delta \tau_d$ which grows with v_d .

Ageing. In a more general approach one has to include ageing of the contacts [5]. Indeed, the threshold value of contact after its reattachment should grow with the time of stationary contact, e.g., because of plastic deformations at the level of contacts or a slow formation of chemical bonds.

Although we do not know the actual ageing mechanism, one may assume that the evolution of newborn thresholds can be represented as a stochastic process described by the simplest stochastic equation $df_{si} =$

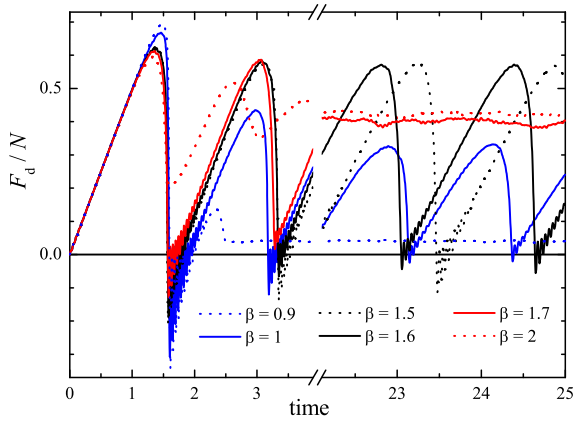


FIG. 8: (color online): The friction force versus time for different values of the ageing rate β (see legend); stick-slip exists for the rates within the interval $1 \leq \beta \leq 1.6$. $f_s = 1$, $\Delta f_s = 0.1$, $\Delta f_0 = 0.01$, $k = 1$, $N = 2 \times 10^3$, $K/N = 1$, $M = 10^{-4}$, $v_d = 1$ and $\eta = 0.1\Omega$.

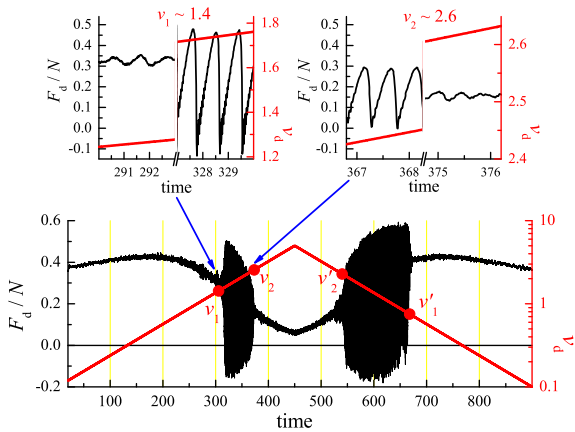


FIG. 9: (color online): The friction force as function of time, when the driving velocity v_d (thick red line, right axes) continuously increases/decreases with time. The insets show the smooth to stick-slip transition at v_1 and the stick-slip to smooth sliding transition at v_2 when v_d increases. $\beta = 1.5$, other parameters as in Fig. 8.

$H(f_{si}) dt + G dw$ with $\langle dw \rangle = 0$ and $\langle dw dw \rangle = dt$, where $H(f)$ and G are the so-called drift and stochastic forces correspondingly [15]. Alternatively, this process is described by the Langevin equation

$$df_{si}(t)/dt = H(f_{si}) + G\xi(t), \quad (13)$$

where $\xi(t)$ is the Gaussian random force, $\langle \xi(t) \rangle = 0$ and $\langle \xi(t)\xi(t') \rangle = \delta(t-t')$. The Langevin equation (13) is equivalent to the Fokker-Planck equation (FPE) for the distribution of thresholds $P_c(f_{si}; t)$:

$$\frac{\partial P_c}{\partial t} + \frac{dH}{df_{si}} P_c + H \frac{\partial P_c}{\partial f_{si}} = \frac{1}{2} G^2 \frac{\partial^2 P_c}{\partial f_{si}^2}. \quad (14)$$

Following Ref. [16], let us assume that the drift force

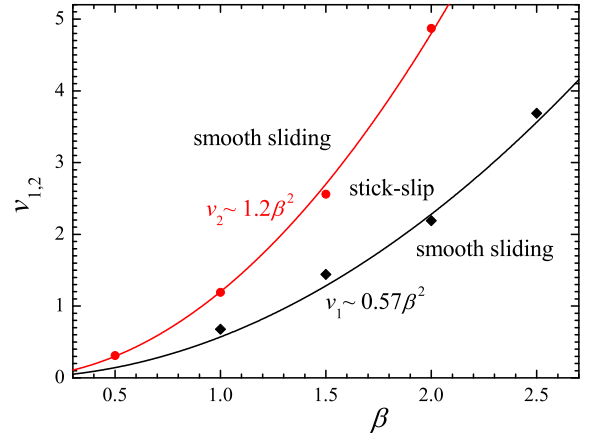


FIG. 10: (color online): The critical velocities v_1 and v_2 as functions of the ageing rate β . Solid curves show fits $v \propto \beta^2$. The parameters as in Fig. 9.

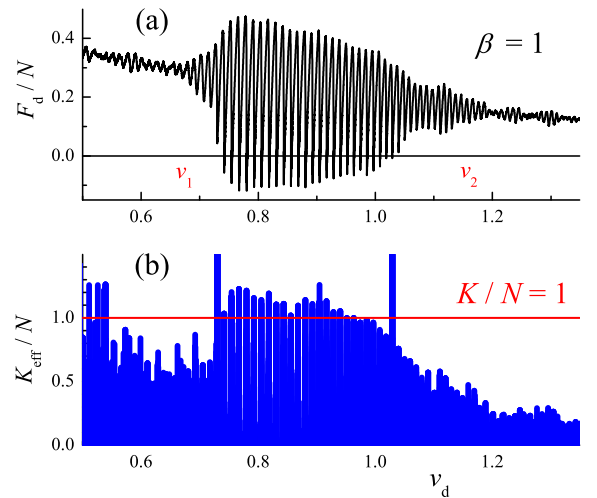


FIG. 11: (color online): (a) The friction force and (b) the effective stiffness K_{eff} as functions of the driving velocity v_d for the ageing rate $\beta = 1$. The parameters are as in Fig. 9.

is given by the expression

$$H(f) = \beta^2 (f_s - f), \quad (15)$$

while the amplitude of the stochastic force is equal to

$$G = \beta \delta f_s \sqrt{2}, \quad (16)$$

where $\delta \equiv \Delta f_s / f_s$ and β defines the rate of ageing described by the timescale $\tau_\beta = \beta^{-2}$. With this choice, the stationary solution $P_{c0}(f)$ of the FPE corresponds to the Gaussian distribution $P_{c0}(f) = (2\pi)^{-1/2} (\delta f_s)^{-1} \exp[-\frac{1}{2}(1-f/f_s)^2/\delta^2]$.

The ME approach described above should now be modified, because the distribution $P_c(x)$ is not fixed but evolve due to ageing of the contacts. Equation (14) describes how the distribution of the thresholds evolves under the effect of ageing alone. This equation may be

rewritten as

$$\frac{\partial P_c}{\partial t} = \beta^2 \hat{L} P_c, \quad \hat{L} = \frac{\partial}{\partial \phi} \left(\phi - 1 + \delta^2 \frac{\partial}{\partial \phi} \right), \quad (17)$$

where $\phi = f/f_s$. However, because the contacts continuously break and form again when the slider moves, this introduces two extra contributions in the equation determining $\partial P_c/\partial t$ in addition to the pure ageing effect described by Eq. (17): a term $P(x; X)Q(x; X)$ takes into account the contacts that break, while their reappearance with the threshold distribution $P_{ci}(x)$ [e.g., $P_{ci}(x) = \delta(x)$] gives rise to the second extra term in the equation. Therefore, the full evolution of $P_c(x; X)$ is described by the equation

$$\begin{aligned} \frac{\partial P_c(x; X)}{\partial X} - \frac{\beta^2}{v} \hat{L} P_c(x; X) + P(x; X) Q(x; X) \\ = P_{ci}(x) \Gamma(X). \end{aligned} \quad (18)$$

In the result we come to the set of equations (1–3, 18).

If now one will drive the slider through an attached spring, then the motion may correspond to either stick-slip or smooth sliding depending on the rate β ; the stick-slip regime appears for the rates within some interval $\beta_1 \leq \beta \leq \beta_2$, while for smaller or larger values of β the motion is smooth (see Fig. 8).

Thus, when the driving velocity continuously increases, the system should undergo two transitions, the smooth to stick-slip transition at v_1 and the stick-slip to smooth sliding transition at v_2 ; if then v_d decreases, one again observes two transitions at v'_2 and v'_1 (see Fig. 9). The critical velocities v_1 and v_2 depend on the ageing rate β as $v_{1,2} \propto \beta^2$ (Fig. 10). Both transitions may be explained in the same way as above, if we remind that $\tau_\beta \sim \tau_d$: the first transition at v_1 occurs when $\tau_\beta > \tau^*$ (provided the instability criterion is satisfied), while the second transition at v_2 takes place when the elastic instability disappears (see Fig. 11).

Conclusion. We presented the detailed study of the stick-slip behavior of the multicontact interface described by the earthquakelike model. The stick-slip emerges because of two factors, both of which are the necessary conditions. First, the driving spring must be soft enough for the elastic instability to emerge. Second, it must be ageing of the interface—the growth of the static threshold with the lifetime of the stationary contact. The first factor is controlled by the dispersion Δx_s of the distribution $P_c(x)$ of the static thresholds. Therefore, using the interface with a large value of $\Delta f_s/f_s$, one may avoid the elastic instability and thus stick-slip. Besides, the value K^* also depends on the distribution of stretchings in the initial state—if one starts with the stationary distribution $Q_s(x)$, the system will stay in the smooth sliding regime forever. Because of the second factor—the contact ageing—the stick-slip exists only for the interval of sliding velocities $v_1 < v_d < v_2$; both boundary velocities $v_{1,2}$ depend on the ageing rate β as $v_{1,2} \propto \beta^2$. Therefore, the stick-slip may also be avoided by an appropriate choice of the operating velocities.

Contrary to the phenomenological approach widely used in description of stick-slip behavior, our approach is based on the model with well defined parameters which may be measured experimentally and even calculated from first principles. However, a weak point of our approach is that we do not know the actual ageing mechanism. Although it is quite hard to study this slow dynamics experimentally as well as with simulation, the problem of interface ageing is very important not only for tribology, but for other topics such as, e.g., seismology [16].

Acknowledgments. We thank M. Peyrard for helpful discussion. This work was supported by the EGIDE/Dnipro grant No. 28225UH and the NASU “RESURS” program.

-
- [1] B.N.J. Persson, *Sliding Friction: Physical Principles and Applications* (Springer-Verlag, Berlin, 1998).
 - [2] O.M. Braun and A.G. Naumovets, *Surf. Sci. Reports* **60**, 79 (2006).
 - [3] R. Burridge and L. Knopoff, *Bull. Seismol. Soc. Am.* **57**, 341-371 (1967).
 - [4] B.N.J. Persson, *Phys. Rev. B* **51**, 13568 (1995).
 - [5] O.M. Braun and J. Röder, *Phys. Rev. Lett.* **88** (2002) 096102.
 - [6] A.E. Filippov, J. Klafter, and M. Urbakh, *Phys. Rev. Lett.* **92**, 135503 (2004).
 - [7] O.M. Braun and M. Peyrard, *Phys. Rev. Lett.* **100** (2008) 125501.
 - [8] O.M. Braun and M. Peyrard, *Phys. Rev. E* **82** (2010) 036117.
 - [9] O.M. Braun and E. Tosatti, *Europhys. Lett.* **88** (2009) 48003.
 - [10] O.M. Braun and E. Tosatti, *Philosophical Magazine* **91** (2011) 3253.
 - [11] H. Yoshizawa, P. McGuiggan, and J. Israelachvili, *Science* **259**, 1305 (1993).
 - [12] I. Barel, M. Urbakh, L. Jansen, and A. Schirmeisen, *Phys. Rev. Lett.* **104**, 066104 (2010).
 - [13] R. Capozza and M. Urbakh, *Phys. Rev. B* **86**, 085430 (2012).
 - [14] K. Brörmann, I. Barel, M. Urbakh, and R. Bennewitz, *Tribol. Lett.* **50** (2013) 3-15
 - [15] C.W. Gardiner, *Handbook of Stochastic Methods for Physics, Chemistry and the Natural Sciences*. Springer-Verlag Berlin Heidelberg 1985, 1997, 2004.
 - [16] O.M. Braun and M. Peyrard, *Phys. Rev. E* **87** (2013) 032808.